

STRUCTURE OF INORGANIC COMPOUNDS

Crystallochemical Features of Ti- and Sb-Rich Nezilovite

R. K. Rastsvetaeva^{a,*}, V. M. Gridchina^a, D. A. Varlamov^b, and S. Jancev^c

^aShubnikov Institute of Crystallography, Federal Scientific Research Centre “Crystallography and Photonics,”
Russian Academy of Sciences, Moscow, 119333 Russia

^bInstitute of Experimental Mineralogy, Russian Academy of Sciences, Chernogolovka, Moscow oblast, 142432 Russia

^cUniversity of Saints Cyril and Methodius, Skopje, Republic of North Macedonia

*e-mail: rast@crys.ras.ru

Received March 22, 2023; revised April 23, 2023; accepted May 2, 2023

Abstract—A variety of the mineral nezilovite, containing antimony and an elevated amount of titanium, has been studied using microprobe and X-ray diffraction analysis. The diffraction experiment was performed on a crystal presenting an aggregate of nezilovite and högbomite with close unit-cell parameters. The parameters of the hexagonal cell of the nezilovite studied are $a = 5.8855(2)$ Å, $c = 23.092(1)$ Å, $V = 692.73(4)$ Å³, sp. gr. $P6_3/mmc$. The structural model is refined using a limited number of unique reflections $231F > 4\sigma(F)$ to $R = 0.08$. The crystallochemical formula is $(Z = 2) \text{PbZn}_2(\text{Ti}_{0.9}\text{Al}_{0.1})(\text{Al}_{0.6}\text{Sb}_{0.4})\text{Mn}_2^{3+}\text{Fe}_6^{3+}\text{O}_{18.5}(\text{O},\text{OH})_{0.5}$. The distribution of cations of this composition over structure sites is established. A basis of the mineral structure is a set of spinel layers, consisting of edge-sharing Fe^{3+} octahedra. They alternate with two heteropolyhedral layers: Zn tetrahedra combine (Al,Sb) octahedra in one layer, and five-vertex Ti polyhedra combine dimers of Mn^{3+} octahedra in the other layer.

DOI: 10.1134/S1063774523700256

INTRODUCTION

Complex oxides of the spinel group are formed in metasomatic ores located within the so-called “Mixed Series” of the Pelagonia massif (Republic of North Macedonia) [1–3]. The interest in these objects is due to the high content of chalcophilic elements (Pb, Zn, Sb, As) with complete absence of sulfides and sulfosalts, which leads to an unusual crystallochemical variety of minerals. Five new minerals have been found in ores of this complex; one of them is nezilovite $\text{PbZn}_2(\text{Mn}^{4+}, \text{Ti}^{4+})_2\text{Fe}_8^{3+}\text{O}_{19}$, found near the village of Nezilovo [4]. It is a zinc representative of the magnetoplumbite group: complex oxides with the general formula $AM_{12}\text{O}_{19}$, where A are large cations (Pb, Ba, Sr, or Ca) and M are small cations with coordination numbers ranging from 4 to 6 (Fe^{3+} , Fe^{2+} , Mn^{4+} , Mn^{3+} , Mn^{2+} , Ti^{4+} , Cr^{3+} , Zn, Mg). The crystallochemical formula of these minerals in the general form is $A^{[XII]}(M1)^{[VI]}(M2)^{[IV]}(M3)_2^{[6]}(M4)^{[6]}(M5)_6^{[6]}\text{O}_{19}$, $Z = 2$ [3]. According to electron microscopy data, crystals shaped as very thin plates (up to ~0.2 mm in the cross section) form syntactic aggregates up to ~0.05 mm thick, consisting of two (sometimes three) minerals, alternating along the c axis. In particular, one can observe coalescence of nezilovite with högbomite $\text{Al}_{18.0}(\text{Fe},\text{Zn})_{5.1}\text{Mg}_{3.9}\text{Ti}_{1.0}\text{O}_{38}(\text{OH})_2$ (sp. gr. $P\bar{3}m1$)

having the trigonal-cell parameters $a = 5.722(1)$ Å and $c = 23.026(4)$ Å [5].

The attention of researchers was attracted by a nezilovite variety of unusual composition, found at another site of the Nezilovo metasomatic complex in the valley of the Babuna river, 40 km southwest of Veles. This part of the complex was formed as a result of the supply of chalcophilic elements at low sulfur activity and high barium activity. These conditions led to the formation of ores of unique type [6].

Nezilovite, as well as högbomite, belongs to the polysomatic series of trigonal (sp. gr. $P\bar{3}m1$) and hexagonal (sp. gr. $P6_3/mmc$) minerals. The systematic (homoaxial) coalescence of this variety of nezilovite with högbomite- $2N3S$ is due to the proximity of the unit-cell parameters of these minerals.

In this work we studied for the first time the crystal chemistry of a nezilovite variety characterized by the presence of antimony and a titanium content twice as high as that in the holotype sample.

EXPERIMENT AND REFINEMENT OF THE STRUCTURAL MODEL

The chemical composition of the samples was studied by electron probe X-ray microanalysis using a scanning electron microscope Tescan Vega-II XMU (EDS mode, accelerating voltage 20 kV, current 400 pA)

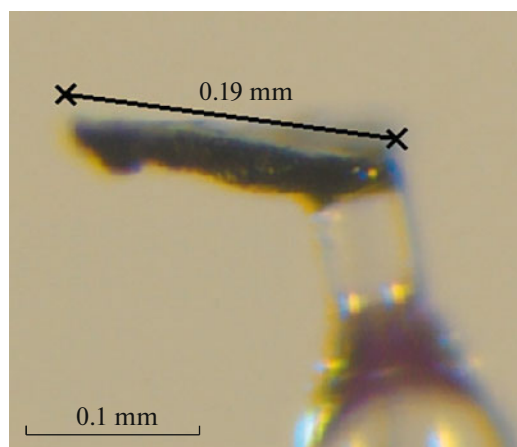


Fig. 1. Fragment of a homoaxial nezilovite intergrowth with a högbomite-supergroup mineral on the holder.

and the INCA Energy 450 system for recording X rays and calculating the sample composition. The electron beam diameter was 157–180 nm. The composition was determined by analyzing the polished surface of a polymineral aggregate, in which nezilovite is present in form of separate lamellae up to 4 μm thick.

Table 1. Crystallographic characteristics, details of the X-ray experiment, and results of structural model refinement

Simplified formula	$\text{PbZn}_2(\text{Ti}_{0.9}\text{Al}_{0.1})(\text{Al}_{0.6}\text{Sb}_{0.4}^{5+})\text{Mn}_2^{3+}\text{Fe}_6^{3+}\text{O}_{18.5}(\text{O},\text{OH})_{0.5}$
$a, c, \text{\AA}$	5.8855(2), 23.092(1)
$V, \text{\AA}^3$	692.73(4)
System, sp. gr., Z	Hexagonal, $P6_3/mmc$, 2
Crystal sizes, mm	$0.19 \times 0.05 \times 0.02$
T , K	293
Diffractometer	XtaLAB Synergy-DW HyPix-Arc 150°
Radiation; λ , \AA	$\text{MoK}\alpha$; 0.71073
Scan mode	ω
Absorption correction; T_{\min}, T_{\max}	Over faceting; 0.341, 0.601
Ranges of indices h, k, l	$-10 \leq h \leq 10, -10 \leq k \leq 10,$ $-38 \leq l \leq 38$
θ_{\max} , deg	75.37
Total number of reflections, R_{av} , number of unique reflections with $F > 4\sigma(F)$	22264, 0.05, 231
Refinement technique	Least-squares method on $ F $
R	0.08
Calculation program	AREN [8]

The calculated empirical formula (the content ranges are indicated with allowance for the grain inhomogeneity), $\text{Pb}_{0.8-1.0}\text{Ca}_{0-0.2}\text{Zn}_{2.1-2.5}\text{Mg}_{0.1}\text{Mn}_{1.8-2.0}\text{Ti}_{0.5-0.9}\text{Sb}_{0.15-0.4}\text{Fe}_{5.6-6.3}\text{Al}_{0.7-1.3}\text{O}_{19}$ ($Z = 2$), shows that this variety of nezilovite is characterized by elevated (in comparison with holotype) content of zinc, titanium, and antimony.

Several samples were selected for X-ray diffraction analysis. According to the results of preliminary experiments, a sample of the best diffraction quality was chosen from a fragment of a syntactic aggregate of nezilovite with a högbomite-group mineral in the form of a thin lamella $0.19 \times 0.05 \times 0.02$ mm in size (Fig. 1). A complete diffraction experiment was performed at a temperature of 293 K using an XtaLAB Synergy-DW X-ray diffractometer with a photon count detector HyPix-Arc 150° (Table 1). The integration of diffraction peaks and correction for the Lorentz factor and radiation polarization were performed using the CrysAlisPro 1.171.42.80a software [7].

The experiment was carried out on a syntactic aggregate of two phases with dominance of the nezilovite component. A cell with hexagonal parameters, corresponding the nezilovite unit cell, was selected: $a = 5.8855(2)$ \AA , $c = 23.092(1)$ \AA , $V = 692.73(4)$ \AA^3 , sp. gr. $P6_3/mmc$. The diffraction experiment yielded 22264 reflections with $F > 4\sigma(F)$, and, after averaging equivalents ($R_{\text{av}} = 0.05$), the dataset contained 360 reflections with $F > 4\sigma(F)$. Despite the fact that 80% detected reflections fit into the nezilovite cell, the reflections corresponding to each of the phases could not be separated, and the model was refined using a limited number (231) of unique reflections with $F > 4\sigma(F)$. Due to the contribution of the second component to the overlapping reflections, the R factor remained at a level of $\sim 8\%$.

When studying the structure, the atomic coordinates in the nezilovite structure were used as a starting dataset [4]. Cations were distributed over model sites based on the composition and multiplicity of sites and the interatomic distances in polyhedra, with allowance for the atomic displacement parameters. The least-squares method was applied to refine the atomic sites and atomic displacement parameters of cations in the anisotropic approximation. An overall isotropic atomic displacement parameter $B_{\text{iso}} = 2$ \AA^2 was fixed for anions. The composition of the $M1$ and $M2$ sites was refined using mixed atomic scattering curves. All calculations were performed using the AREN software [8]. The final atomic coordinates and characteristic atomic displacements are listed in Table 2, and the interatomic distances and the composition of polyhedra are given in Table 3.

The structural model contains layers consisting of tetrahedra, five-vertex polyhedra, and octahedra. The presence of zinc in tetrahedra was beyond doubt, whereas the distribution of cations over sites in five-vertex polyhedra and octahedra was complicated

Table 2. Atomic coordinates, isotropic atomic displacement parameters (B_{iso}), and Wyckoff positions (Q)

Site	x/a	y/b	z/c	Q	$B_{\text{iso}}, \text{\AA}^2$
<i>A</i>	2/3	1/3	1/4	2 <i>d</i>	2.58(19)
<i>M1</i>	0	0	0	2 <i>a</i>	0.75(49)
<i>M2</i>	0	0	1/4	2 <i>b</i>	1.0(2)
<i>M3</i>	1/3	2/3	0.0242(2)	4 <i>f</i>	0.69(25)
<i>M4</i>	2/3	1/3	−0.1898(2)	4 <i>f</i>	0.51(30)
<i>M5</i>	0.1689(8)	0.339(1)	−0.1062(1)	12 <i>k</i>	0.85(13)
O1	0	0	0.156(1)	4 <i>e</i>	2.0
O2	1/3	2/3	−0.049(1)	4 <i>f</i>	2.0
O3	0.361(1)	0.180(1)	3/4	6 <i>h</i>	2.0
O4	0.143(4)	0.285(5)	0.053(1)	12 <i>k</i>	2.0
O5	0.500(3)	−0.500(3)	0.351(1)	12 <i>k</i>	2.0

Table 3. Characteristics of coordination polyhedra

Site	Composition ($Z = 2$)	CN	Cation–anion distances, \AA		
			minimum	maximum	average
<i>A</i>	Pb _{1.0}	12	2.88(1)	2.94(1)	2.91
<i>M1</i>	Al _{0.6} + Sb _{0.4} ⁵⁺	6	1.90(2)	1.90(2)	1.90
<i>M2</i>	Ti _{0.9} + Al _{0.1}	5	1.84(1)	2.16(2)	1.97
<i>M3</i>	Zn ₂	4	1.68(2)	2.05(2)	1.95
<i>M4</i>	Mn ₂ ³⁺	6	1.94(1)	2.084(4)	2.01
<i>M5</i>	Fe ₆ ³⁺	6	1.94(2)	2.13(1)	2.02

CN is the coordination number.

because of the almost identical M –O distances in them. With allowance for the scattering power of atoms, dominance of Fe³⁺ in the octahedra of the spinel layer and Al in the octahedra of the polyhedral layer was established. Mn³⁺ atoms fill the octahedra of the other polyhedral layer.

Despite the relatively low accuracy of determining interatomic distances, the reliability of cation distribution over structural model sites was proven by calculating the bond–valence sum [9] (Table 4). The increased valence values for iron and manganese atoms (3+) and for antimony (5+) is confirmed by the oxidative situation in the Pelagonia massif.

DESCRIPTION AND DISCUSSION OF THE STRUCTURE

The main specific features of the composition and structure of the mineral manifest themselves in its crystallochemical formula ($Z = 2$), which is in good correspondence with the empirical one: Pb^[XII](Zn₂)^[IV](Ti_{0.9}Al_{0.1})^[IV](Al_{0.6}Sb_{0.4}⁵⁺)^[VI](Mn₂³⁺)^[VI]–

(Fe₆³⁺)^[VI]O_{18.5}(O,OH)_{0.5}, where the Roman numerals in square brackets denote the coordination numbers of atoms. The simplified formula of the mineral can be written as ($Z = 2$) PbZn₂(Ti_{0.9}Al_{0.1})(Al_{0.6}Sb_{0.4}⁵⁺)(Mn₂³⁺)₂Fe₆³⁺O_{18.5}(O,OH)_{0.5}.

The nezilovite structure consists of ten layers, oriented perpendicular to the c axis of the hexagonal cell (Fig. 2). Four layers consist of Fe octahedra, connected over edges into six-membered rings, with Fe–O distances lying in the range of 1.94(2)–2.13(1) \AA (Fig. 3a). Two layers contain vertex-sharing octahedra and tetrahedra in a ratio of 1 : 1 (Fig. 3b). The tetrahedra contain zinc, with Zn–O distances ranging from 1.68(2) to 2.05(2) \AA , while octahedra are occupied by Al; Al–O = 1.90(2) \AA . The enlarged distances in the Al octahedron are due to the incorporation of larger antimony atoms into it, which amount to 40% of the mixed composition. Both tetrahedral and octahedral coordinations are characteristic of aluminum, in which it forms diverse structures: from discrete octahedra to frameworks. For example, in the structure of tashelgite (oxide of complex composition and struc-

Table 4. Bond–valence sums

Site	O1	O2	O3	O4	O5	V_{cat}
Zn		$1.07 \times 1 \rightarrow$ $\times 1 \downarrow$		$0.39 \times 3 \rightarrow$ $\times 1 \downarrow$		2.24
Fe ³⁺	$0.43 \times 1 \rightarrow$ $\times 3 \downarrow$	$0.34 \times 1 \rightarrow$ $\times 3 \downarrow$		$0.47 \times 2 \rightarrow$ $\times 2 \downarrow$	$0.61 \times 2 \rightarrow$ $\times 2 \downarrow$	2.90
Mn ³⁺			$0.41 \times 3 \rightarrow$ $\times 2 \downarrow$		$0.60 \times 3 \rightarrow$ $\times 1 \downarrow$	3.03
Al _{0.6} ³⁺ Sb _{0.4} ⁵⁺				$0.51 \times 6 \rightarrow$ $0.90 \times 6 \rightarrow$ $0.70_{\text{cp}} \times 1 \downarrow$		3.06 5.40
Ti ⁴⁺	$0.39 \times 2 \rightarrow$ $\times 1 \downarrow$		$0.96 \times 3 \rightarrow$ $\times 1 \downarrow$			3.66
Pb ²⁺			$0.11 \times 6 \rightarrow$ $\times 2 \downarrow$		$0.13 \times 6 \rightarrow$ $\times 1 \downarrow$	1.44
V_{an}	1.68	2.09	2.00	2.03	1.95	

The valence strengths on an anion–cation bond are given in rows for cations and in columns for anions. The summation directions are indicated by arrows. The integer factors correspond to the number of bonds made by a given cation with symmetry-equivalent anions or a given anion with symmetry-equivalent cations.

ture) [10], the role of aluminum is diverse. Al atoms occupy sites in tetrahedra (the Al–O distance is in the

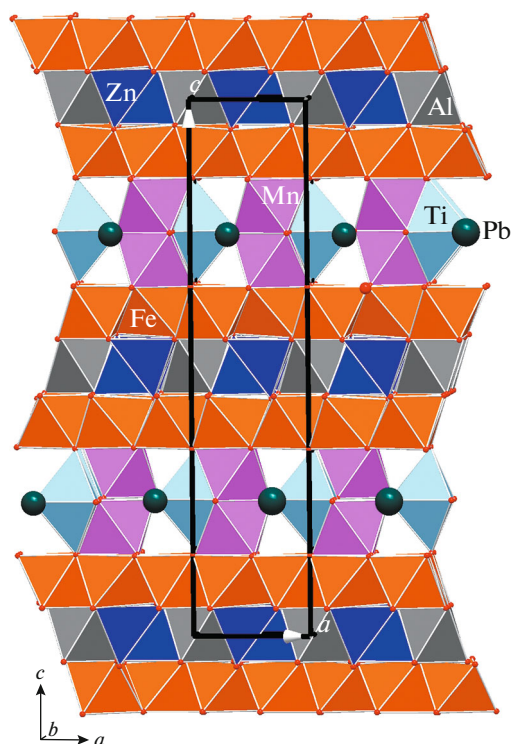


Fig. 2. General view of the nezilovite structure along the c axis.

range of 1.65–1.85 Å) and mainly in octahedra with the distances Al–O = 1.68–2.14 and 1.76–2.06 Å.

Octahedral and heteropolyhedral layers, being connected via vertices and edges of polyhedra, form blocks characteristic of the structures of spinel and minerals of the högbomite polysomatic series. In högbomite-group minerals spinel blocks (S blocks) regularly alternate with nolanite-type blocks (N blocks) in different ratios [5]. The polyhedral layer in an N block consists of octahedra and tetrahedra in a ratio of 1 : 1; it is topologically similar to the nezilovite layer in the projection onto the (001) plane (Fig. 4a). Despite the fact that the heteropolyhedral layers of nezilovite and högbomite have the same appearance in this projection, the nezilovite layer structure is different: with the axis 3 inclined, one can see that octahedra share faces to combine into dimers, and there are five-vertex polyhedra instead of tetrahedra (Fig. 4b). Merging of two heteropolyhedral layers of a nolanite block and its subsequent transformation lead to the formation of a large cavity in the nezilovite structure. This cavity is occupied by Pb in the 12-vertex polyhedron with distances in the range of 2.88(1)–2.94(1) Å, which is the main difference in the compositions of both minerals.

The differences in the compositions of the nezilovite variety studied here from the nezilovite holotype [4] concern mainly the cation distribution over the double layer sites. In particular, the five-vertex polyhedron of the investigated mineral contains Ti (with a small Al impurity), with Ti–O distances lying in the range of 1.84(1)–2.16(2) Å, whereas the octahedron contains Mn³⁺ with the distances Mn³⁺–O = 1.94(1)–2.084(4) Å. In the face-shared octahedra the distance

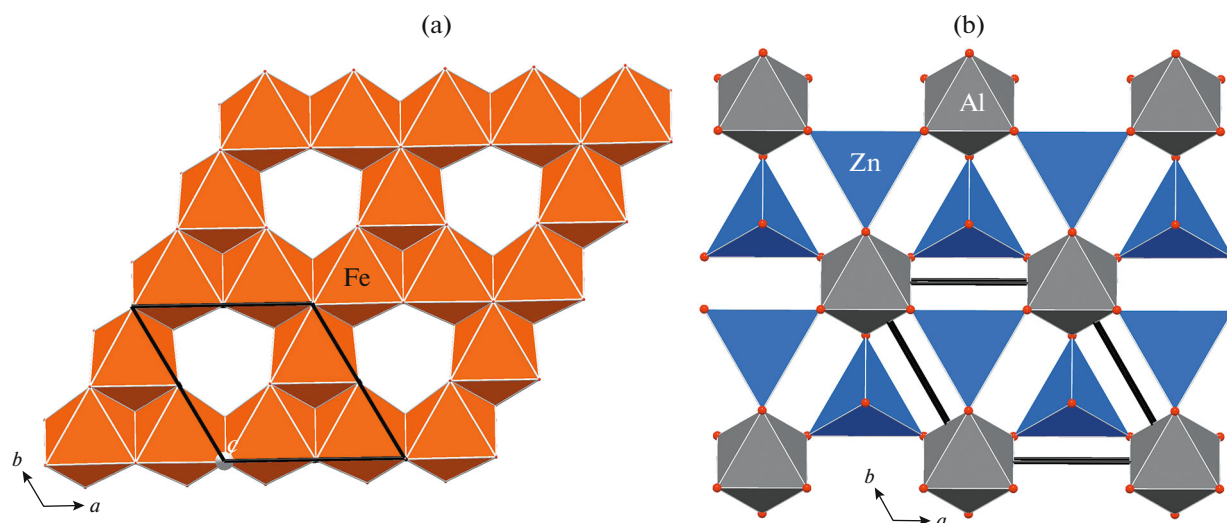


Fig. 3. Fragments of the nezilovite structure projected onto the (001) plane: (a) octahedral layer and (b) polyhedral layer composed of tetrahedra and octahedra.

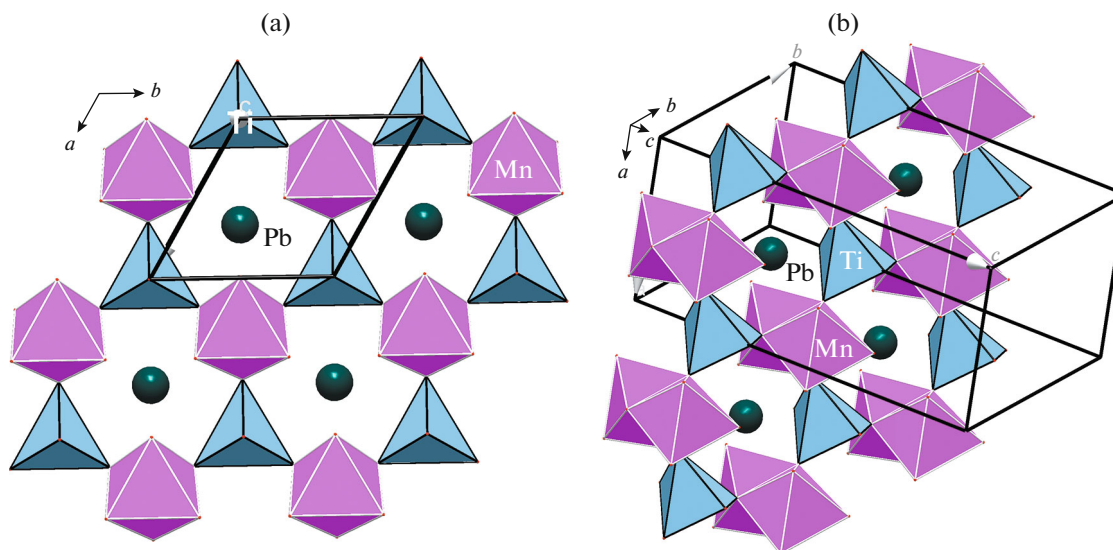


Fig. 4. Fragment of the nezilovite structure: (a) a layer composed of five-vertices and octahedral dimers in projection onto the (001) plane and (b) in a prospective view.

between the cations centering them, $\text{Mn}^{3+}-\text{Mn}^{3+}$, is smaller than 3 Å and amounts to 2.78(1) Å. In the holotype nezilovite sample [4], the five-vertex polyhedron with the distances 1.84(2)–2.46(2) Å is occupied by Fe^{3+} with a small impurity of Mn^{4+} , and the octahedron contains Mn^{4+} and Ti, whereas Mn^{3+} is located in the octahedral layer, along with Fe^{3+} . As was shown above, the M1 octahedron in the spinel-block polyhedral layer in both minerals is occupied by Al; in the holotype this octahedron is entirely occupied by Al; and, in the investigated mineral, characterized by a

smaller amount of Al and a high content of Sb, these elements supplement each other.

CONCLUSIONS

The results of the X-ray diffraction study of a sample of nezilovite intergrown with högbomite-2N3S allow us to state that the obtained model adequately describes the chemical composition and cation distribution over structure sites. This gives grounds to use further the found model in structure refinement according to the diffraction data for a single crystal.

If single-crystal samples of titanium-rich nezilovite or nezilovite with a high antimony content will be found, this model will be interesting for studying the corresponding, potentially new minerals.

Since magnetoplumbite-group minerals possess ferrimagnetic properties, which have a technical application potential, the presence of antimony may affect these properties. An analysis of the Sb-containing nezilovite variety and the information on the antimony site in the mineral structure may be useful when synthesizing materials with magnetic properties.

ACKNOWLEDGMENTS

We are grateful to N.V. Chukanov for supplying crystals and participation in the discussion of the results.

FUNDING

The study was performed using equipment of the Shared Research Center of the Federal Scientific Research Centre “Crystallography and Photonics” of the Russian Academy of Sciences within the State assignment of the Ministry of Science and Higher Education of the Russian Federation for the FSRC “Crystallography and Photonics” RAS.

CONFLICT OF INTEREST

The authors declare that they have no conflicts of interest.

REFERENCES

1. N. V. Chukanov, S. Jančev, and I. V. Pekov, *Macedonian J. Chem.* **34** (1), 115 (2015).
<https://doi.org/10.20450/mjccce.2015.612>
2. V. N. Ermolaeva, D. A. Varlamov, S. Yanchev, and N. V. Chukanov, *Zap. Vseross. Mineral. O-va* **147** (3), 27 (2018).
<https://doi.org/10.30695/zrmo/2018.1473.02>
3. N. V. Chukanov, S. S. Vorobei, V. N. Ermolaeva, et al., *Zap. Vseross. Mineral. O-va* **147** (3), 44 (2018).
<https://doi.org/10.30695/zrmo/2018.1473.03>
4. V. Bermanec, D. Holtstam, and D. etSturman, *Can. Mineral.* **34**, 1287 (1996).
5. C. Hejny and Th. Armbruster, *Am. Mineral.* **87**, 277 (2002).
<https://doi.org/10.2138/am-2002-2-309>
6. S. Jančev, *Geol. Maced.* **17** (1), 59 (2003).
7. *Rigaku Oxford Diffraction, 2022, CrysAlisPro Software System, Version 1.171.42.80a* (Rigaku Oxford Diffraction, Yarnton, UK).
8. V. I. Andrianov, *Kristallografiya* **34** (3), 592 (1989).
9. I. D. Brown and D. Altermatt, *Acta Crystallogr. B* **41**, 244 (1985).
<https://doi.org/10.1107/S0108768185002063>
10. R. K. Rastsvetaeva, S. M. Aksenov, and I. A. Verin, *Dokl. Chem.* **434**, 233 (2010).
<https://doi.org/10.1134/S0012500810090065>

Translated by Yu. Sin'kov